JVI Journals.ASM.org

A Histidine Residue of the Influenza Virus Hemagglutinin Controls the pH Dependence of the Conformational Change Mediating Membrane Fusion

Caroline M. Mair,[a] Tim Meyer,[b] Katjana Schneider,[a] Qiang Huang,[c] Michael Veit,[d] Andreas Herrmann[a]

Molecular Biophysics, Institute of Biology, Humboldt University, Berlin, Germany[a]; Macromolecular Modeling, Institute of Chemistry and Biochemistry, Free University, Berlin, Germany[b]; State Key Laboratory of Genetic Engineering, School of Life Sciences, Fudan University, Shanghai, China[c]; Cell Biology of Viral Infections, Institute of Virology, Free University, Berlin, Germany[d]

ABSTRACT

The conformational change of the influenza virus hemagglutinin (HA) protein mediating the fusion between the virus envelope and the endosomal membrane was hypothesized to be induced by protonation of specific histidine residues since their pK_as match the pHs of late endosomes (pK_a of ~6.0). However, such critical key histidine residues remain to be identified. We investigated the highly conserved His184 at the HA1-HA1 interface and His110 at the HA1-HA2 interface of highly pathogenic H5N1 HA as potential pH sensors. By replacing both histidines with different amino acids and analyzing the effect of these mutations on conformational change and fusion, we found that His184, but not His110, plays an essential role in the pH dependence of the conformational change of HA. Computational modeling of the protonated His184 revealed that His184 is central in a conserved interaction network possibly regulating the pH dependence of conformational change via its pK_a. As the propensity of histidine to get protonated largely depends on its local environment, mutation of residues in the vicinity of histidine may affect its pK_a. The HA of highly pathogenic H5N1 viruses carries a Glu-to-Arg mutation at position 216 close to His184. By mutation of residue 216 in the highly pathogenic as well as the low pathogenic H5 HA, we observed a significant influence on the pH dependence of conformational change and fusion. These results are in support of a pK_a-modulating effect of neighboring residues.

IMPORTANCE

The main pathogenic determinant of influenza viruses, the hemagglutinin (HA) protein, triggers a key step of the infection process: the fusion of the virus envelope with the endosomal membrane releasing the viral genome. Whereas essential aspects of the fusion-inducing mechanism of HA at low pH are well understood, the molecular trigger of the pH-dependent conformational change inducing fusion has been unclear. We provide evidence that His184 regulates the pH dependence of the HA conformational change via its pK_a. Mutations of neighboring residues which may affect the pK_a of His184 could play an important role in virus adaptation to a specific host. We suggest that mutation of neighboring residue 216, which is present in all highly pathogenic phenotypes of H5N1 influenza virus strains, contributed to the adaptation of these viruses to the human host via its effect on the pK_a of His184.

Infection by enveloped viruses requires fusion of the viral membrane with the cellular target membrane to release their genome into the cell cytoplasm (1, 2). For influenza virus, upon endocytic uptake, the virus fuses with the endosomal membrane. Fusion is mediated by a conformational change of the viral hemagglutinin (HA) which is triggered in the acidic milieu of late endosomes (2, 3). Both the prefusion and essential features of the postfusion structure of HA consisting of two covalently linked subunits (HA1 and HA2) are known (4, 5). Protonation-induced opening of the interfacial contacts of the HA1 globular head is considered the initiating step of the conformational change (6, 7). As a consequence, water can enter the central cavity, which in turn induces the structural transitions of the fusion-triggering subunit HA2 (6). These include formation of a long helix and insertion of the N-terminal fusion peptide at the tip of this helix into the target membrane (2, 3, 5, 8, 9).

Whereas essential steps of the fusion-mediating conformational change of HA are well understood, specific amino acids that have to be protonated to induce the structural rearrangements remain essentially unknown. Histidines have been proposed to function as such molecular "switches" in class I and II viral fusion proteins due to their unique characteristics to become protonated and thus charged in the same acidic pH range within which these viral proteins are activated (pK_a of ~6.0) (10–17). Kampmann et al. identified potential pH-sensing histidines by a high degree of conservation and the position at specific locations, such as proximity to other positively charged residues or colocation with other histidines (10). Based on that, four highly conserved histidines were suggested as potential triggers of the HA conformational change at low pH: HA1 residue His184 and HA2 residues His106/His111, His142, and His159 (10). However, only His106 of the H3 subtype and the corresponding His111 of the H5 subtype have been analyzed in detail but with contradictory results (13, 18, 19). Whereas computational modeling revealed that protonation of

Received 12 June 2014 Accepted 27 August 2014
Published ahead of print 3 September 2014
Editor: A. García-Sastre
Address correspondence to Andreas Herrmann, andreas.herrmann@rz.hu-berlin.de.

doi:10.1128/JVI.01704-14

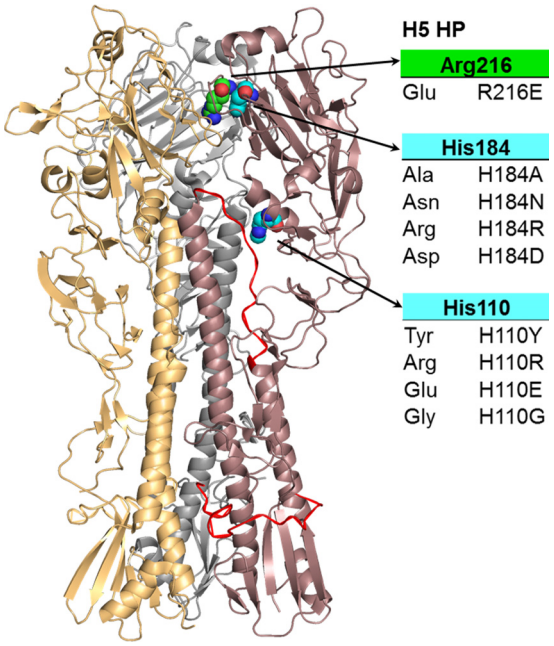

FIG 1 Crystal structure of the highly pathogenic H5 HA in surface and cartoon representation (PDB ID 2IBX). Monomers are marked in brown, orange, and gray. Histidines at positions 184 and 110 (cyan) as well as the residue at position 216 (green) are depicted as spheres in the brown monomer with selected substitutions listed in the table. The fusion peptide and the B-loop are highlighted in red.

His106/His111 induces bending of peptides corresponding to a small part of the long helix of H1 and H3 subtypes (19), mutation of these histidines in H3 (13) as well as in H5 HA (18) barely had any effect on fusion and its pH threshold. Furthermore, except for His184, all of the above suggested histidines are located in the fusion domain of HA and might be involved in later steps of the conformational change. Thus, there is no experimental evidence for histidines which, upon protonation, trigger early steps of the HA conformational change, such as the dissociation of HA1 monomers.

We focus here on His184 as a potential molecular switch (8) triggering the conformational change of HA. Indeed, due to its central position at the HA1-HA1 interface, protonation of His184 very likely could destabilize intermonomeric prefusion contacts upon protonation (Fig. 1). Furthermore, His184 is highly conserved among all subtypes (except H17 and H18) and within individual subtypes, emphasizing its significance. Likewise, we addressed His110 as a potential pH sensor at the HA1-HA2 interface of H5 HA as it is part of the 110-helix close to the B loop which is rearranged at low pH (20, 21). His110 may trigger structural rearrangements of this domain upon its protonation. However, His110 is conserved only in the H2, H5, H13, and H16 subtypes. To test the role of His110 and His184 as pH-dependent triggers of the conformational change, we replaced these two histidines with a set of different amino acids in the highly pathogenic H5 subtype (H5 HP) and analyzed the mutant proteins for conformational change and fusion. The structural consequences of mutations were rationalized by computational modeling.

Since the propensity of histidines to get protonated depends on their local environment (presence of other proton-donating residues, hydrophobic shielding, and interaction with other residues), the pK_a of individual histidines such as His184 or His110 can be altered by mutations in close proximity (10, 16, 17). Comparing the sequences of highly pathogenic and low pathogenic H5 (H5 LP) HA proteins, we identified a glutamate-to-arginine mutation at position 216 in proximity to His184 at the HA1-HA1 interface. Such mutations altering the pH of fusion have been reported in several studies to modulate H5N1 virus pathogenicity in the avian as well as the mammalian host (22–26). An altered pH sensitivity of H5 HA due to mutation at position 216, as we reason, might be the result of a pK_a-modulating effect on His184. To unravel a potential effect on the pK_a of His184, we substituted Glu216 for Arg (E216R) in the low pathogenic H5 HA and Arg216 for Glu (R216E) in the highly pathogenic H5 HA.

MATERIALS AND METHODS

Plasmids and viruses. H5 HA from A/chicken/Vietnam/P41/2005 (H5 HP wild type [wt]) and viral RNA from low pathogenic H5N1 (A/teal/Germany/Wv632/2005) (H5 LP wt) were obtained from the Friedrich Loeffler Institute, Riems, Germany. Viral RNA was transcribed to cDNA using the Uni12 primer (AGCAAAAGCAGG) and subsequently amplified with H5-specific forward and reverse primers (27). The sequences encoding the H5 LP and HP HA proteins were cloned into a pCAGGS expression plasmid using the Esp3I (Fermentas) restriction enzyme and T4 DNA ligase (Fermentas) according to the method of Czudai-Matwich et al. (28). Point mutations were introduced by site-directed mutagenesis using an overlap extension PCR and were verified by DNA sequencing. All amino acid residues are numbered according to the H3 subtype.

Transient expression of HA proteins. Monolayers of CHO cells were grown in Dulbecco's modified Eagle's medium (DMEM) supplemented with 10% fetal bovine serum (FBS), 2 mM glutamine, and 1% penicillin-streptomycin (DMEM full medium). For transient expression of the HA proteins at the cell surface, CHO cells were transfected with pCAGGS HA using the transfection reagent Turbofect (Fermentas) according to the manufacturer's instructions. Transfected CHO cells were incubated for 24 h for fusion analysis and for 48 h for the assessment of expression and conformational change in DMEM full medium at 37°C and then treated as indicated below for each experiment.

Cleavage activation of H5 LP HA. HA is synthesized as the HA0 precursor protein which needs to be cleaved into HA1 and HA2 after trimerization for subsequent fusion studies. Highly pathogenic HA (H5 HP HA) proteins carry a polybasic cleavage site which is cleaved by intracellular proteases in the course of transport to the cell surface. In contrast, low pathogenic HA (H5 LP HA) proteins have a monobasic cleavage site which can be cleaved only extracellularly by trypsin-like proteases. Thus, before acidification, the H5 LP HA wild-type and E216R mutant proteins were treated with 4 μg/ml tosylsulfonyl phenylalanyl chloromethyl ketone (TPCK)-trypsin for 5 min at room temperature for cleavage activation.

Adjustment of pH *in vitro*. The pH of the fusion buffer (10 mM HEPES, 10 mM morpholineethanesulfonic acid [MES], and 100 mM NaCl in phosphate-buffered saline [PBS] containing magnesium and calcium [PBS+]) was adjusted with 1 M NaOH and 1 M HCl before the buffer was added to the HA-expressing cell monolayers. In the red blood cell (RBC) fusion assay, cells were incubated for 5 min with fusion buffer at the respective pH at 37°C with a subsequent reneutralization step for 2 min at 37°C. For conformational change analysis by flow cytometry, cell monolayers were incubated for 15 min with fusion buffer before reneutralization.

Red blood cell fusion assay. Fresh human red blood cells (RBCs) were doubly labeled with the lipoid dye octadecyl rhodamine B chloride (R18) and the content marker calcein (Molecular Probes/Life technologies) as described previously (29, 30). HA-expressing CHO cells were treated with 0.5 U/ml neuraminidase from *Clostridium perfringens* (Sigma) and (if required) with 4 μg/ml TPCK-trypsin (Sigma), followed by incubation

with DMEM supplemented with 10% FBS. CHO cells carrying cleaved HA proteins were then incubated with the doubly labeled RBCs for at least 30 min to allow for binding of the RBCs to HA at the cell surface. Then, samples were washed to get rid of unbound RBCs and analyzed for fusion at low (pH 5.0 to 6.6) and high (pH 7.0) pHs under a fluorescence microscope (Olympus Fluoview FV-1000).

Trimer formation assay. Trimer formation of H5 wild-type and mutant proteins was determined by SDS-PAGE and Western blotting using the cross-linker 3,3-dithiobissuccinymidylpropionate (DSP) and the monoclonal anti-H5 Vn04-2 antibody (dilution of 1:1,000; Rockland Immunochemicals) (18, 31). At 48 h posttransfection cells were lysed and centrifuged (12,000 × *g* for 5 min), and supernatants were treated with 0.8 mM DSP in dimethyl sulfoxide (DMSO) for 15 min at 15°C. The reaction was stopped by addition of 20 mM ammonium chloride, and after the loading dye was added and samples were boiled for 5 min, they were subjected to SDS-PAGE and Western blot analysis under nonreducing conditions. Equal loading of wells was confirmed by Western blotting with a mouse monoclonal primary antibody against the cellular protein β-actin (dilution, 1:3,000; Sigma).

Immunostaining and flow cytometry. Expression of the HA proteins at the cell surface was analyzed at neutral pH using the Vn04-2 antibody (dilution, 1:1,000). The conformation of HA at different pHs was assessed using the monoclonal antibodies Vn04-9 and Vn04-16 (31) (dilution, 1:500; Rockland Immunochemicals) according to Reed et al. (18). Transfected CHO cells growing in 24-well plates were incubated at neutral (pH 7.0) or low (pH 5.0 to 6.6) pH for 15 min at 37°C. After reneutralization with PBS+ medium, cell monolayers were blocked with 0.2% bovine serum albumin (BSA) in PBS+ for 15 min and placed on ice. For expression analysis, cells were overlaid with the primary antibody Vn04-2, whereas for assessing the conformational change, primary antibodies Vn04-9 and Vn04-16 were used. After incubation for 45 min, samples were washed three times with 0.2% BSA in PBS+ and overlaid with a fluorescently labeled secondary anti-mouse antibody for 30 min. Cells were detached using 2 mM EDTA in PBS following analysis by flow cytometry using a FACS Aria II instrument (BD Biosciences). Expression of mutant proteins relative to the wild type was evaluated by normalizing the median fluorescence intensity (MFI) values of 10,000 cells to that of the highly pathogenic H5 HA wild-type protein. The pH of conformational change was determined as the point at which a 50% change in signal occurred between the minimum and maximum of the respective Vn04-9/Vn04-16 ratios.

Structural modeling of mutant proteins. The modeled protein structures are based on the crystal structure of the highly pathogenic H5 HA (Protein Data Bank identification number [PDB ID] 2IBX). The His184 residues in chains A, C, and E were replaced. Missing atoms were added using default internal coordinates of CHARMM22 (32, 33). To obtain reasonable interactions of the mutated residue with its environment, the model was geometry optimized with CHARMM (33) using the CHARMM22 (32) force field. The influence of the solvent was considered implicitly with a dielectric constant of 80 by using the module generalized Born with simple switching (GBSW) (33) of the CHARMM program. To obtain the correct protonation state for histidines at neutral pH, an electrostatic energy calculation was performed using the software Karlsberg+ (34).

Statistical analysis. Graphing and statistical analysis were performed by using GraphPad Prism, version 5 (GraphPad software, San Diego, CA). For comparison of two samples, an independent *t* test was applied (see Fig. 4). For the statistical comparison of multiple data sets, a one-way analysis of variance (ANOVA) with Dunnett's multiple comparison posttest was used (see Fig. 2 and 3). Probability values of less than 0.05 were considered statistically significant.

RESULTS

Selection of substitutes for histidine. For characterization as potential molecular switches, we replaced His184 and His110 with different amino acids and analyzed their effects on conformational change and fusion (Fig. 1). Previous mutational studies of histidines (H17 and H106/H111) in the HA protein revealed that the effect on fusion largely depends on the substituted amino acids (13, 18, 35). Thus, in order to obtain comprehensive results, we selected a subset of structurally diverse amino acids as substitutes for His184 and His110. Asparagine was selected to replace His184 (H184N). It is structurally most similar to histidine and thus might be able to interact with neighboring residues at the interface similar to histidine but does not have the propensity to get protonated at low pH. In contrast, the neutral alanine at position 184 (H184A) was predicted to abrogate any interactions of His184 with neighboring residues, which would provide information about the structural significance of histidine at position 184. Arginine with its positive charge was selected to mimic a protonated histidine which, at first glance, should destabilize intermonomeric interactions. The negatively charged aspartate was chosen as a residue potentially stabilizing the HA1-HA1 interface. Correspondingly, we selected arginine as destabilizing (H110R), glycine as neutral (H110G), and glutamate as stabilizing (H110E) substitutes for His110. Tyrosine (H110Y) was selected due to its reported stabilizing effect on H5 HA when the histidine at position 110 was replaced (36, 37).

Cell surface expression and trimerization of mutant proteins. Any mutation introduced can also interfere with other processes unrelated to the pH threshold of fusion-mediating conformational changes such as protein folding, oligomerization, intracellular transport, or maturation. Specifically, the highly conserved histidine at position 184 might be indispensable for correct protein folding. Therefore, we analyzed trimer formation and cell surface expression of H5 HP and LP HA mutants (Fig. 2). By using the cross-linking reagent DSP, we detected trimers for all variants. Hence, mutation of His184, His110, and residue 216 does not seem to affect the ability of H5 HA to trimerize. Cell surface expression was quantified by immunostaining and flow cytometry using the specific anti-H5 antibody Vn04-2 (18, 31, 38), which served also as an indication of correct protein folding. In general, substitution of His184 had a more pronounced effect on HA expression than substitution of His110 or mutation of residue 216. H184R and H184D mutants exhibited significantly higher (H184R) or lower (H184D) cell surface expression levels than the H5 HP HA wild type (P values of <0.001 and 0.01, respectively), whereas mutants H184N and H184A were expressed at levels similar to the wild-type level. His110 as well as the H5 LP HA E216R and the H5 HP HA R216E mutants was also similarly expressed; only the low pathogenic H5 HA showed significantly higher expression than the wild type (P values of <0.05). Although the extent of surface expression was different, correct protein folding of surface-expressed HA was indicated by antibody Vn04-2 binding, trimerization, and binding of RBCs (see below) to HA-expressing cells for all generated mutants.

Effect of mutations on fusion. To assess the effect of histidine mutations in HA of H5 HP on the pH of fusion, we used a well-established red blood cell (RBC) fusion assay (29, 30, 39–41). Before binding to HA-expressing cells, RBCs were labeled with a membrane (R18; red) and a content marker (calcein; green). Only full fusion of membranes represented by redistribution of both dyes to an HA-expressing cell upon low-pH incubation was evaluated as a fusion event. The hemifusion intermediate characterized by lipid/R18 mixing without content/calcein mixing was ob-

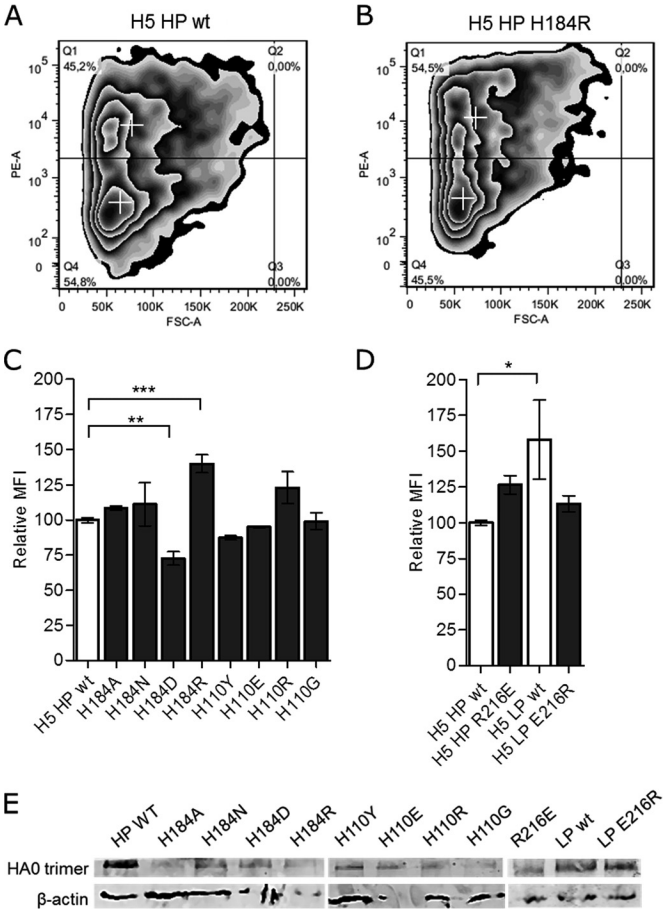

FIG 2 Cell surface expression of wild-type and mutant HA proteins of H5 HP and LP. Cell surface expression of mutant proteins was quantified by immunostaining and flow cytometry using the H5-specific antibody Vn04-2. (A and B) Representative images of flow cytometry measurements using the highly pathogenic wild-type protein (A) and the H184R mutant protein (B). Gate Q1 represents the fluorescent positive cells of each measurement compared to the mock control, with red crosses indicating the median fluorescence intensity of the respective gate. FSC-A, forward scatter, area; PE-A, phycoerythrin, area. (C and D) The median fluorescence intensity (MFI) value of fluorescent cells (gate Q1) in each sample was normalized to that of the H5 HP HA wild-type protein (relative MFI). Error bars represent the standard errors of the means from triplicate experiments. Significant differences are marked by asterisks with probability determined by one-way ANOVA and Dunnett's multiple comparison posttest: *, $P < 0.05$; **, $P < 0.01$; ***, $P < 0.001$. (E) Trimer formation of histidine mutants and of highly pathogenic and low pathogenic H5 HA with mutation at position 216. HA trimers and the cellular protein β-actin were detected by SDS-PAGE and Western blotting following incubation with the cross-linking agent DSP.

served only in rare cases and was not rated as a fusion event. The pH of fusion corresponds to the highest pH at which full fusion was still observed for at least 50% of HA-expressing cells. Mutation of His184 to Asn (H184N) and Ala (H184A) shifted the pH of fusion from 5.8 to 6.2 and 6.4, respectively, whereas mutation to Asp (H184D) and Arg (H184R) abolished fusion of H5 HP HA even at pH 5.0 (Fig. 3A). For H184D the low cell surface expression of the mutant, which is also indicated by the low level of RBC binding, might explain the absence of fusion at low pH. In contrast, the H184R mutant showed high surface expression and thus higher levels of red blood cell binding than the wild-type protein but still did not induce fusion. Thus, despite its positive charge, which was predicted to disrupt the interfacial contacts, arginine at position 184 seems to inhibit the fusion-mediating conformational change of HA.

Mutation of His110 did not show any effect on the pH of fusion except for the histidine-to-tyrosine change (H110Y). This shifted the fusion pH from 5.9 to 5.6, as already reported (36). However, analysis of the crystal structure of the H110Y mutant (37) indicated that the stabilizing effect of tyrosine at position 110 cannot be explained by the absence of histidine but by an additional hydrogen bond at the HA1-HA2 interface which is formed with residue Asn413. Thus, since replacement of His184 but not of His110 had a major impact on the pH of fusion, we investigated in detail only the role of His184 for the conformational change of HA.

Effect of His184 mutations on the conformation of HA at neutral and acidic pHs. Monoclonal antibodies Vn04-9 and Vn04-16 (31) were reported to preferentially bind to the neutral (Vn04-9) or the low-pH (Vn04-16) conformation of surface-expressed H5 HA (18, 22). We used these two conformation-specific antibodies to determine the pH of the conformational changes of H5 mutants. Median fluorescence intensity (MFI) values of fluorescent HA-expressing cells, which were incubated at pHs ranging from 5.0 to 7.4 and reneutralized before immunostaining, were measured and normalized to the maximal MFI obtained with the respective antibody (relative MFI). We found significant pH-dependent binding for only the Vn04-9 antibody, whereas binding of antibody Vn04-16 remained rather constant at all pH values analyzed. Therefore, the ratio of Vn04-9 to Vn04-16 reactivity was calculated (see Materials and Methods) and plotted as a function of pH (Fig. 3B). The pH of conformational change was determined as the point at which a 50% change in the antibody binding ratio was observed. Shifts in the pH of conformational change obtained for the mutant proteins relative to the wild type were compared to those observed for fusion with RBCs (Fig. 3C). Mutations to alanine and asparagine resulted in shifts in the pH of conformational change of +0.5 and +0.2 units, respectively, similar to the results of the RBC assay. Also for the H184D mutant we observed a decrease in the ratio with the lowering of the pH. Data indicate an increase in the pH threshold of conformational change of 0.5 units, similar to the H184A mutant. However, we note that the change in the ratio of antibody binding activity of H184D is moderate compared to that of the wild-type HA and mutants H184N and H184A (Fig. 3B). For H184R we did not observe a pH dependence of binding, indicating that this mutant does not undergo a conformational change. This is supported by the failure to trigger fusion.

Effect of the residue at position 216 on fusion and conformational change of HA. The HA proteins of highly pathogenic H5N1 strains, which caused massive bird die-offs associated with sporadic spillover infections to humans and other mammals in the 2003-2004 outbreak (42, 43), carry arginine residues at position 216, whereas HAs of low pathogenic strains have glutamates at this position. To test if the insertion of an opposite charge in proximity to His184 modulates the pH of fusion, we mutated arginine to glutamate in the highly pathogenic H5 HA (H5 HP HA R216E) and glutamate to arginine in the low pathogenic H5 HA (H5 LP HA E216R). The pHs of conformational change and of fusion with labeled RBCs for wild-type and mutant proteins were measured as described in Materials and Methods, and the obtained data were normalized to the value for the wild-type HA of H5 HP (Fig. 4).

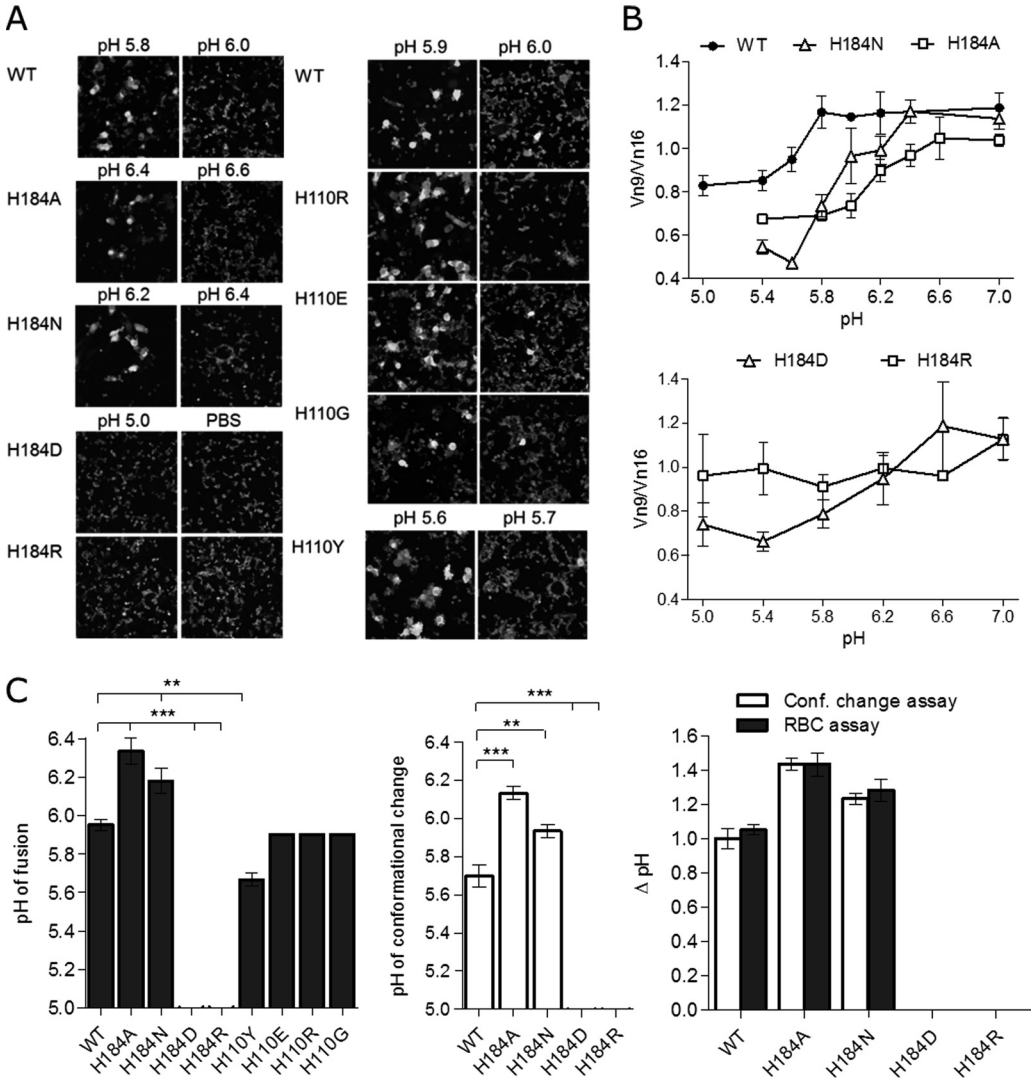

FIG 3 pH of conformational change and of fusion for histidine mutants of HA (H5 HP). (A) Representative images of the RBC fusion assay for wild-type (WT) and histidine mutant H5 HA proteins expressed at the CHO cell surface. Only full fusion of membranes represented by redistribution of both the membrane marker (R18; red) and content marker (calcein; green) from RBCs to the HA-expressing cells following incubation at the indicated pH at 37°C was rated as a fusion event. The pH of fusion was generally assessed in steps of 0.2 pH units. Since for the His110 mutants there was no change in the pH of fusion compared to that of the wild type (except H110Y), a 0.1-pH-unit resolution for these mutant proteins was used. (B) The conformational change of the wild-type and His184 mutant proteins was assessed by plotting the obtained Vn04-9/Vn04-16 ratios of median fluorescence intensities as a function of pH. The average and standard errors are shown ($n \geq 3$). (C) Summary of data obtained from the RBC fusion and the conformational change assays illustrated in panels A and B, respectively. The pH of fusion corresponds to the highest pH at which full fusion was still observed for at least 50% of HA-expressing cells ($n \geq 3$). The pH of conformational change corresponds to the pH of 50% change of Vn04-9/Vn04-16 antibody ratio obtained from median fluorescence intensities. In the right panel, the differences in the pH shift of fusion and conformational (Conf) change of His184 mutants relative to the wild-type HA are shown. Error bars represent the standard errors of the mean. Statistical difference based on one-way ANOVA and Dunnett's multiple comparison posttest is indicated as follows: *, $P < 0.05$; **, $P < 0.01$; ***, $P < 0.001$.

Mutation of residue 216 had a significant effect on the pH of conformational change for both the highly pathogenic and the low pathogenic H5 HAs. The replacement of arginine with glutamate (positive against negative charge) in H5 HP HA caused an increase of 0.2 units, whereas the glutamate-to-arginine mutation (negative against positive charge) in the H5 LP HA produced a change in the pH threshold of conformational change of −0.4 units. The pH of fusion of the highly pathogenic H5 HA was also significantly increased by the exchange of charge at position 216 (+0.3 units). Although not statistically distinguishable in the H5 LP HA, a change of −0.2 units in the fusion pH was detected when the Glu-to-Arg mutation was introduced.

DISCUSSION

His184, a determinant of the pH dependence of the conformational change of HA. In several studies, histidines have been discussed as pH-dependent triggers of conformational change of viral fusion proteins because their protonation state changes from uncharged to positively charged in the acidic environment of endosomes (44–46). Mutational studies on different class II viral

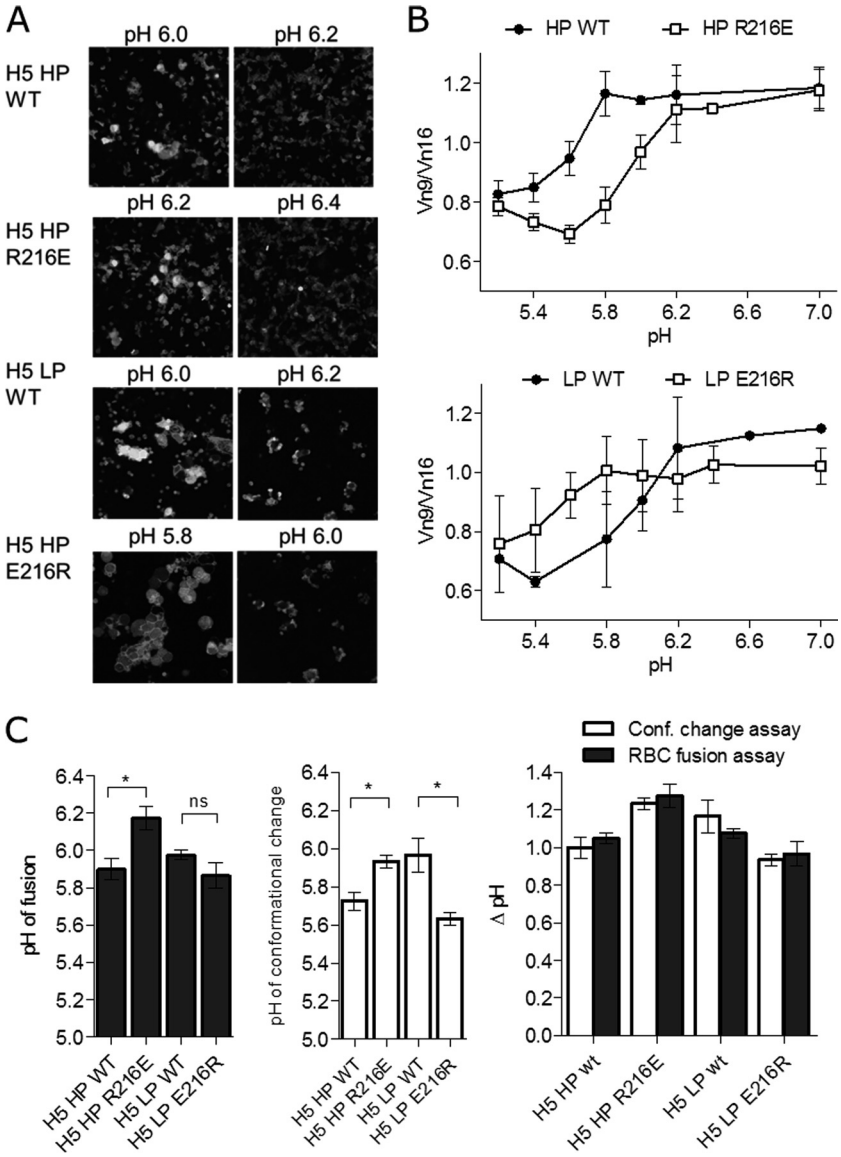

FIG 4 Effect of a mutation of opposite charge at position 216 on the pH dependence of fusion and of conformational change of H5 HP and H5 LP HA proteins, respectively. (A) Representative images of the RBC fusion assay for H5 HP and LP wild-type HAs and respective mutant proteins after incubation at the indicated pH at 37°C ($n \geq 3$). (B) pH-dependent conformational change of H5 HP and LP wild-type HAs and mutant proteins as detected by antibody binding and flow cytometry. Vn04-9/Vn04-16 ratios of median fluorescent intensities were plotted as a function of pH. The average and standard errors are shown ($n \geq 3$). (C) Summary of data obtained from the RBC fusion and the conformational change assays illustrated in panels A and B, respectively. The pH of fusion of the wild-type and mutant proteins as assessed by the RBC fusion assay at 37°C corresponds to the highest pH at which full fusion of membranes could still be detected ($n \geq 3$). The pH of conformational change corresponds to the pH of 50% change of the antibody Vn04-9/Vn04-16 ratio obtained from median fluorescence intensities. In the right panel, the differences in the pH shift of fusion and conformational change in relation to the highly pathogenic wild type are shown. Error bars represent the standard errors of the means. Statistical difference was determined by an independent *t* test (*, $P < 0.05$; ns, nonsignificant).

fusion proteins such as the E protein of tick-borne encephalitis virus (47) and the E1 protein of Semliki Forest virus (48) have provided evidence of specific histidines as critical pH sensors. The aim of our study was to characterize His184 at the HA1-HA1 interface and His110 at the HA1-HA2 interface of influenza virus HA as potential molecular switches. We replaced both histidines by a set of different amino acids in the highly pathogenic H5 HA and analyzed the mutational effect on pH-dependent conformational change and fusion. Except for tyrosine, mutation of His110 did not affect the pH dependence of either the conformational change or fusion. The H110Y mutation was already previously shown to stabilize HA at this position owing to an additional hydrogen bond (36, 49). Apparently, the altered pH of fusion was not due to the absence of histidine but to the interaction of tyrosine with Asn413 of the adjacent monomer (49). Therefore, we do not consider His110 as a trigger of conformational change.

In contrast to findings for His110, we found a significant impact of mutating His184 on the pH dependence of conformational change and fusion. Mutation of His184 either abrogated the ability of HA to undergo a fusion-triggering conformational change or shifted the pH dependence of conformational change and fusion to a higher pH, as summarized in Table 1. In general, the pH

TABLE 1 Summary of data obtained for histidine mutants and for highly pathogenic and low pathogenic H5 HA containing a mutation at position 216

HA protein	Surface expression[a] (mean ± SD)	ΔpH[b]		
		RBC fusion assay	Conformational change assay	Avg
H184A	109 ± 2	+0.5	+0.5	+0.5
H184N	111 ± 27	+0.3	+0.2	+0.3
H184D	73 ± 13	—	+0.5	+0.5[c]
H184R	140 ± 14	—	—	
H110Y	87 ± 2	−0.3	ND	−0.3
H110R	123 ± 22	0.0	ND	0.0
H110E	95 ± 1	0.0	ND	0.0
H107G	99 ± 10	0.0	ND	0.0
H5 HP wt	100 ± 5	5.9	5.7	5.8
H5 HP R216E	127 ± 13	+0.3	+0.2	+0.3
H5 LP wt	158 ± 73	6.0	6.0	6.0
H5 LP E216R	113 ± 13	−0.2	−0.4	−0.3

[a] Relative (%) MFI.
[b] The values represent the average from a minimum of three experiments. In all cases the difference between the three measurements did not exceed 0.1 pH units. ND, not determined; —, no fusion or conformational change was detected at any pH.
[c] Only a possible conformational change was detected. See Results and Discussion.

of conformational change measured by antibody binding and flow cytometry was lower than the pH of fusion. The difference could be explained by the assumption that the number of activated HA molecules required to induce fusion is lower than that corresponding to the midpoint of change in the Vn04-9/Vn04-16 ratio, which was defined as the pH of conformational change. Replacing His184 with asparagine and alanine caused a shift to a higher pH for the conformational change of H5 HA and fusion. Mutation of His184 to arginine totally abolished conformational change and fusion. Fusion was also not observed for H184D. This might be related to the significantly lower expression of the mutant on the plasma membrane of CHO cells. Another explanation could be a conformational change that was not able to mediate fusion or even the absence of any conformational change at all. Indeed, although we observed a decrease in the ratio of antibody binding by lowering the pH, the decrease was rather moderate, lacking a sharp decline as observed, for example, for the wild type.

Interaction of His184 and respective mutants as the molecular basis for pH sensing. To gain insight into the structural basis for an altered pH of conformational change and fusion due to mutation of His184, we performed computational modeling of the neutral pH crystal structure of the highly pathogenic wild-type H5 HA (PDB ID 2IBX). We addressed the influence of mutations of His184 on interaction with neighboring residues and, in turn, possible consequences for the pH-dependent stability of the HA ectodomain.

In the wild-type H5 HA, His184 forms an intramonomeric salt bridge with glutamate at position 231 (Fig. 5A and D). Interestingly, a pair of positively charged arginine residues (Arg220 and Arg229) is located close to His184 at the interface of HA1 monomers. Being shielded from water, the two charged amino acids need to be stabilized by a defined number of hydrogen bonds inside the protein which are mostly formed with the backbone amides of neighboring residues of the same monomer (Fig. 5B and C). Arg220 thereby interacts with the backbone of His184 and with the side chain oxygen of Asn210 from the adjacent monomer. These hydrogen bonds are at the same time the only intermonomeric interactions in this region. HA, especially the association of HA1 monomers clamping the HA2 subunit at neutral pH, is metastable so that small alterations at the HA1-HA1 interface could affect the stabilization of the complex, leading to the fusion-inducing conformational change. We surmise that at low pH His184 becomes doubly protonated and thus competes with Arg220 for hydrogen bonding, resulting in the destabilization of the structure and thus in the HA conformational change. By modeling of the doubly protonated His184 into the H5 HP HA crystal structure, we could indeed confirm that protonation may cause His184 to interact with Asn210, thereby weakening the hydrogen bond network of Arg220 (Fig. 5E).

Modeling of the different amino acids at position 184 in the H5 HP HA structure supports the hypothesis of His184 controlling the pH dependence of the conformational change at low pH (Fig. 6). In the case of alanine at position 184, no interaction of this amino acid with surrounding residues occurs. However, as the smallest amino acid, it leaves enough space for water to enter the hydrophobic cavity, which possibly weakens the interfacial interactions in general. Asparagine as well as aspartate at this position forms a hydrogen bond with Asn210 in the neutral-pH structure. As a result these residues have a strong influence on the hydrogen bond network of Arg220 and Arg229 near the intermonomeric interface, suggesting a destabilizing effect of these mutations. While for asparagine this is in line with our experimental results, for aspartate we could not observe fusion, and we noted only a possible conformational change with rather moderate pH dependence. This result illustrates and supports the high sensitivity of this region to the character of the amino acid present at position 184. Aspartate and asparagine are structurally very similar, and thus both are able to form a hydrogen bond with Asn210, as shown by computational modeling. However, due to its negative polarity, aspartate might have a different effect than asparagine on the stability of the complex, which we are not able to predict.

According to our experimental studies, arginine at position 184 prevents a conformational change of HA which is, at a first glance, an unexpected observation. Arginine is positively charged like a protonated histidine, and the latter is thought to support the dissociation of the monomers due to ionization. In contrast, as revealed by modeling of the H184R mutation, the arginine at position 184 forms a double salt bridge with Glu231 which is very stable. Furthermore, the polar atoms of the long residue are most distant from Asn210 and Arg220 and closer to the surrounding water, which may result in a much weaker influence on the hydrogen bond network of Arg220 and Arg229 residues than the mutations or substitutes discussed before (H184A, H184N, H184D). Taken together, except for H184D, our modeling approach allows a rationalization of the molecular basis for the influence of His184 mutations on the respective pH shift of the conformational change of HA and fusion.

His184 is part of a conserved interaction network at the HA1-HA1 interface. In order to investigate the significance of Arg220, Arg229, and Asn210 in triggering the conformational change, we aligned the HA sequences of subtypes from H1 to H18 (Table 2). Both arginine residues (R220 and R229) are highly conserved. Residue 210 is also partly conserved as it is an asparagine, glutamine, threonine, or serine in all subtypes. These amino acids are all structurally similar and polar, enabling their interaction with Arg220. The only exceptions to the consensus interactions at the

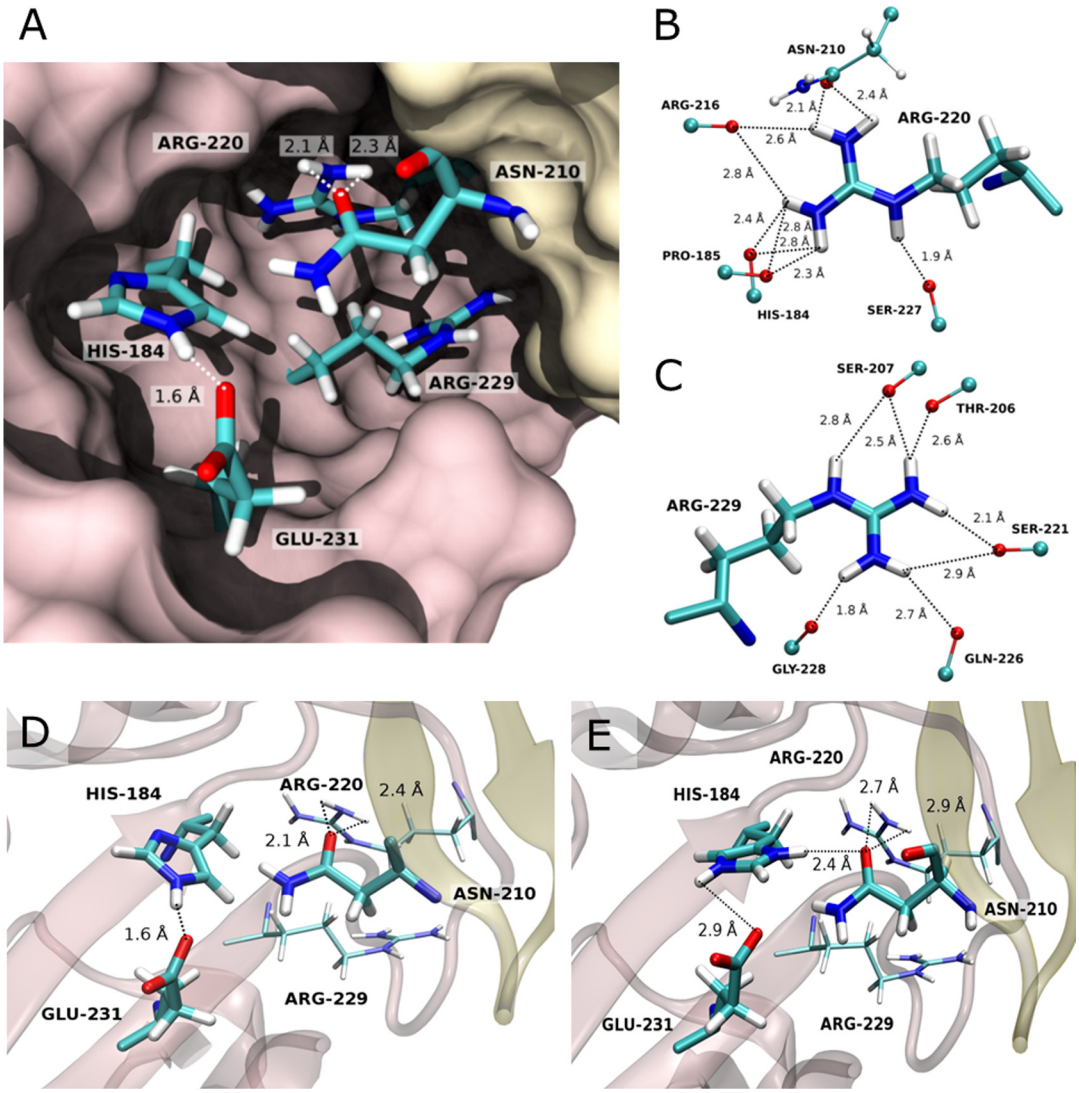

FIG 5 Interactions of His184 and of neighboring residues at the HA1-HA1 interface in its neutral (A and D) and doubly protonated (E) states (PDB ID 2IBX). (A) Interactions at the HA1-HA1 interface. Monomers (chain A in brown and chain E in yellow) are depicted in surface representation, and residues which might be crucial for the regulation of HA1 monomer dissociation are shown in stick model. (B and C) Hydrogen bond network of residues Arg220 and Arg229. Interactions are formed between the polar atoms of residues Arg220 (B) and Arg229 (C) with those of the backbone amides, except for Asn210, where the hydrogen bond is formed with the side chain carbonyl-oxygen. The hydrogens were modeled as described in Materials and Methods. (D and E) Crystal structure of the HA1-HA1 interface at neutral pH (PDB ID 2IBX) (D) and its modeled conformation upon protonation of His184 at a pH below 5 (E). Secondary structures of chains A (brown) and E (yellow) are displayed in cartoon representation with residues His184, Arg216, Glu231, and Asn210 in stick model. For the modeling, the side chain of His184 has been rotated by 180 degrees, and the structure has been subsequently energy minimized. We suggest that a strong hydrogen bond is formed between His184 and Asn210, while the interaction between Asn210 and Arg220 is significantly weakened.

HA1-HA1 interface are the four subtypes of newly defined group 3 of HAs (H13, H16, H17, and H18) (50–52). H13 and H16 carry tryptophan at position 229. However, both have lysines at position 231 which might compensate for the "lost" Arg229. In bat-derived H17 and H18, position 184 is an asparagine and a glutamine, respectively. These two subtypes were suggested to have a different mechanism of fusion activation and might not necessitate a pH-dependent conformational change of HA (51–53). Thus, the absence of histidine at position 184 in the H17 and H18 subtypes in contrast to its high degree of conservation not only between but also within all other subtypes reinforces the requirement of a histidine at position 184 for the pH-dependent conformational change of histidine.

According to our results, histidine is the only amino acid at position 184 which is able to stabilize or destabilize the HA1 monomers depending on its pH of protonation, explaining its high degree of conservation in all subtypes (except for H17 and H18). Other residues at position 184 were shown to destabilize (Ala, Asn, and perhaps Asp) the associated HA1 monomers already at a higher subacidic pH (>6.0) or to completely stabilize the HA1-HA1 interface (Arg), abrogating a conformational change and fusion even at rather low pH values. Thus, we suggest that His184 is not the sole trigger of fusion but one determinant regulating the HA conformational change at low pH, as has also been suggested for critical histidines of the West Nile virus E protein (46). Furthermore, the fact that the interactions of Arg229 (or

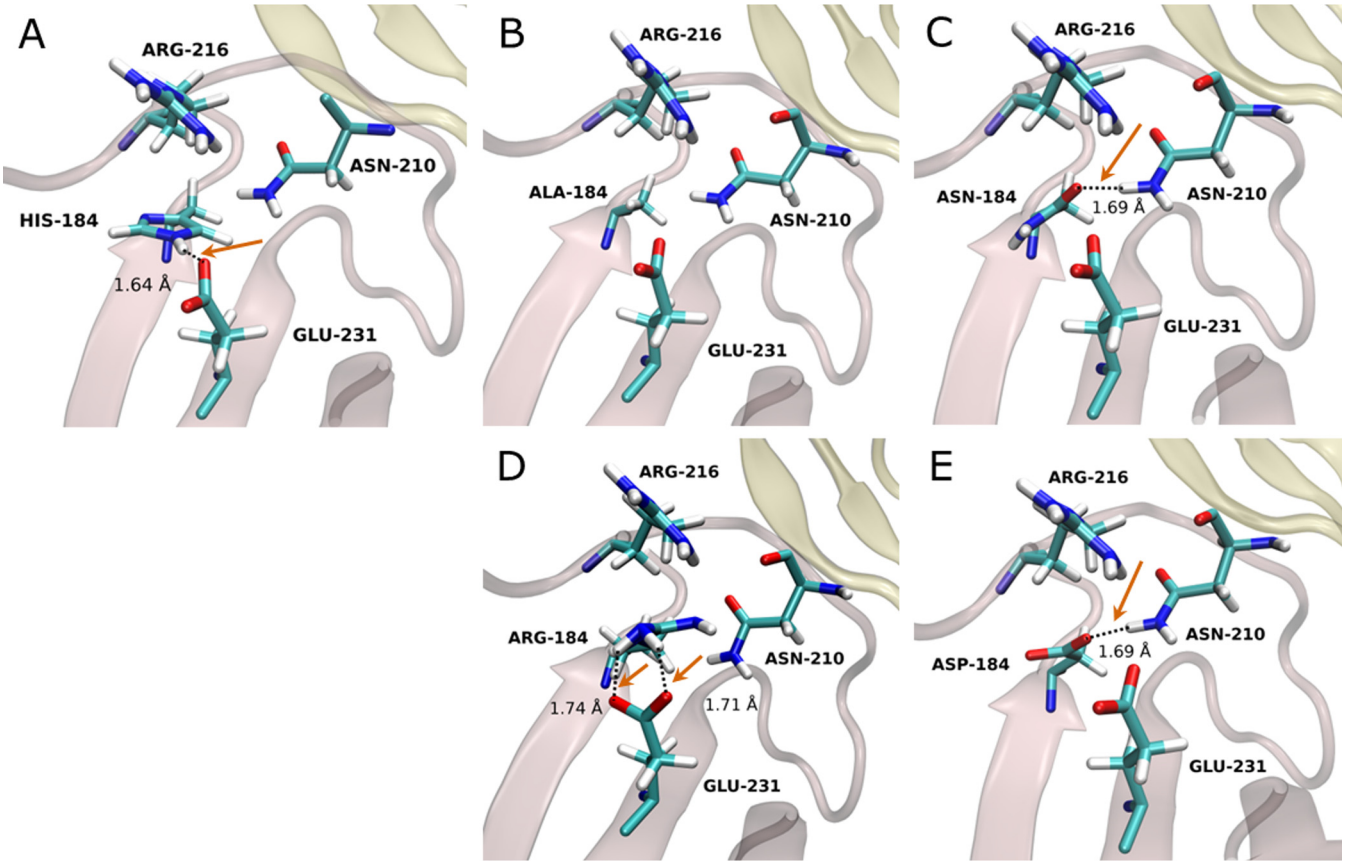

FIG 6 Structural representation of the HA1-HA1 interface of the crystal structure of the H5 HP HA wild type (A) and of modeled mutations at position 184 (B to E). Secondary structures of chains A (brown) and E (yellow) are shown in cartoon representation, with central residues of the interface represented in stick model. Interactions of the respective residues at position 184 are displayed (marked by arrows). For modeling, the His184 residues in chains A, C, and E were replaced by alanine (H184A) (B), asparagine (H184N) (C), arginine (H184R) (D), and aspartate (H184D) (E).

Lys231), Arg220, His184, and residue 210 (and 231) are also conserved indicates that these residues are also crucial for the pH-dependent stability of HA.

Fine-tuning of the pK_a of His184 and regulation of fusion. To obtain the protonation state of His184 at neutral pH, we performed an electrostatic energy calculation using Karlsberg+ (34) based on the crystal structure of H5 HP HA (PDB ID 2IBX, resolved at pH 6.5). We obtained a pK_a value for His184, which is below −10. Since the HA structure with charged histidines is not known, the real pK_a of His184 cannot be predicted accurately using this approach, and the obtained value very likely does not correspond to the actual pK_a of this residue. However, the result clearly indicates that (i) His184 is deprotonated in the crystal structure at pH 6.5 as shown in Fig. 4D, (ii) that His184 is therefore very likely deprotonated also at neutral pH, and (iii) that its pK_a is below 6.5. Due to the complexity of the structural changes that are expected to follow the protonation, the accurate prediction of the pK_a of His184 is a challenging task that we leave open for future investigation.

As His184 is partially buried in the protein, its pK_a depends on the residues in its local environment; i.e., it can be strongly affected and, thereby, precisely adjusted by those residues and by mutations thereof (16, 17). We identified a glutamate-to-arginine mutation at position 216 in the highly pathogenic H5 HA which evolved in 2003 to 2004, killing not only a large number of birds but also humans and other mammals. Residue 216 is located at the HA1-HA1 interface in the vicinity of His184, suggesting that it may affect the pK_a of His184. Although our experimental data do not provide direct evidence, they support this hypothesis. We found that a glutamate instead of arginine at position 216 increases the pH threshold of the conformational change and fusion, whereas replacing glutamate by arginine in the low pathogenic subtype resulted in a decrease in the pH threshold (Table 1). The obtained data correlate with the previously described pK_a dependency of histidines on neighboring residues (10, 14–17). An additional negative charge is known to support protonation of histidine, resulting in an increased pK_a, whereas in the environment of a positively charged residue, the protonated and thus positively charged form is less favored, shifting its pK_a to lower values. Thus, we suppose that the exchange of charge at position 216 causes an alteration of the pH of the conformational change and, consequently, of fusion via its effect on the pK_a of His184. In support of our study, an increase in the pH of fusion when residue 216 was changed from a lysine, which is positively charged like arginine, to glutamic acid (K216E) was reported previously for a highly pathogenic H5 subtype (22). However, the authors argued that the effect of this K216E mutation on the pH of fusion was due to a change in hydrogen bonding with the adjacent monomer (from K216-N210 to E216-R212) (22). Analyzing the known crys-

TABLE 2 Sequence alignment of subtypes H1 to H18 with PDB IDs and UniProtKB accession numbers[c]

Strain	PDB ID	Accession Nr	HA1 sequence in H3 numbering												
			180	181	182	183[a]	184	195	210	215	216[b]	220	221	229	231[b]
H1N1	4JTV	C3W5S1	W	G	I	H	**H**	Y	**S**	P	**E**	**R**	P	**R**	**N**
H2N2	2WR0	D0VWP8	W	G	I	H	**H**	Y	**N**	P	**E**	**R**	P	**R**	**E**
H3N2	1HGD	P03438	W	G	I	H	**H**	Y	**Q**	P	**N**	**R**	P	**R**	**S**
H4N6		M1UPL4	W	G	V	H	**H**	Y	**Q**	P	**N**	**R**	P	**R**	**S**
H5N3	1JSM	A5Z226	W	G	I	H	**H**	Y	**N**	P	**E**	**R**	P	**R**	**E**
H5N1	2IBX	Q45ZQ3	W	G	I	H	**H**	Y	**N**	P	**R**	**R**	S	**R**	**E**
H6N5		F2P1Y8	W	G	V	H	**H**	Y	**N**	P	**E**	**R**	P	**R**	**D**
H7N9		D0FI67	W	G	I	H	**H**	Y	**Q**	P	**S**	**R**	P	**R**	**D**
H7N3	4BSG	Q6GYW3	W	G	I	H	**H**	Y	**Q**	P	**S**	**R**	P	**R**	**D**
H8N4		G2TWE4	W	G	I	H	**H**	Y	**N**	P	**N**	**R**	P	**R**	**D**
H9N2	1JSD	Q91CD4	W	G	I	H	**H**	Y	**N**	P	V	**R**	P	**R**	**D**
H10N7		M1UTF6	W	G	I	H	**H**	Y	**Q**	P	V	**R**	P	**R**	**D**
H11N6		P04661	W	G	I	H	**H**	Y	**N**	P	**E**	**R**	P	**R**	**T**
H12N5		P03446	W	A	I	H	**H**	Y	**N**	P	**N**	**R**	P	**R**	**D**
H13N6	4KPQ	P13103	W	G	I	H	**H**	Y	**S**	L	**E**	**R**	P	W	**K**
H14N5		P26136	W	G	V	H	**H**	Y	**Q**	P	**N**	**R**	P	**R**	**S**
H15N8		Q82565	W	G	V	H	**H**	Y	**Q**	P	**S**	**R**	P	**R**	**D**
H16N3	4F23	Q5DL24	W	G	I	H	**H**	Y	**S**	L	**E**	**R**	I	W	**K**
H17N10	4H32	H6QM93	W	G	I	H	N	Y	**S**	P	**D**	**R**	D	**R**	**D**
H18N11	4MC5	U5N1D3	W	G	V	H	Q	Y	**T**	L	V	**S**	S	**R**	**N**

[a] Highly conserved His183 is involved in receptor binding.
[b] Subtype-specific residues at positions 216 and 231 potentially influence the pK_a of His184.
[c] HA subtypes are listed in alphabetical order. Important residues at the HA1-HA1 interface are shown in boldface. Residues forming the conserved interactions at the HA1-HA1 interface are highlighted.

tal structures (PDB IDs 3S11 and 3S13), we could not identify any of the mentioned hydrogen bonds.

We propose that His184 and its local environment are important determinants for the fine-tuning of the pH of fusion, an essential step of the infection cascade. Several studies have provided evidence that the pH of fusion is crucial for influenza virus infection in distinct organisms (23–25). It was further shown that viral adaptation to different host cells and species often necessitates mutations in the HA protein, altering the fusion pH to account for host-specific variations in the endosomal pH and/or for different transmission modes (36, 54–58). In particular, it has been shown that a high pH of fusion increases the pathogenicity of the virus in infected chicken and ducks (22, 24), whereas a high pH is not favorable for infection of and spread between mammals (23, 25, 36, 54, 55, 58).

Sequence alignment of H5 HAs of isolated H5N1 strains revealed that the glutamate-to-arginine (or lysine) mutation is present in all highly pathogenic virus strains isolated from birds and humans not only in 2003 to 2004 but also in subsequent years, suggesting that the charge-charge mutation and the altered pH of fusion involved contributed to a highly pathogenic phenotype. We propose that this E216(R/K) mutation stabilizes the HA ectodomain of H5 HP, shifting the fusion-triggering conformational change to a more acidic pH. The mutation might also have compensated for other destabilizing mutations, preventing conformational change of H5 HP HA at elevated pH (22).

In conclusion, we suggest that His184 is a crucial molecular switch at the HA1-HA1 interface regulating the pH dependence of the conformational change of HA. We further propose that mutation of residue 216 in proximity to His184 alters the pH threshold of conformational change and of fusion by affecting its pK_a. This fine-tuning of the pK_a of His184 may facilitate the adaptation of the fusion pH to host-specific conditions, which was shown to be required for efficient infection and spread of the virus.

ACKNOWLEDGMENTS

We thank Thomas Mettenleitner (Friedrich Loeffler Institute, Insel Riems, Germany) for providing the cDNA of highly pathogenic H5 HA and RNA of low pathogenic H5 HA, Volker Czudai-Matwich (Phillips University, Marburg, Germany) for providing the pCAGGS plasmid, Charles J. Russell (St. Jude's Children Hospital, Memphis, TN) for his expertise in immunostaining with conformation-specific antibodies, and Christian Sieben and Roland Schwarzer (Humboldt University Berlin) for critical readings and discussions.

This work was supported by the European Union (ITN Marie Curie Virus Entry, to C.M.M. and Q.H.) and the DFG (SFB 765 to T.M., SFB 740 to M.V., and HE 3763/15 to A.H.).

REFERENCES

1. **Kielian M, Rey FA.** 2006. Virus membrane-fusion proteins: More than one way to make a hairpin. Nat. Rev. Microbiol. **4:**67–76. http://dx.doi.org/10.1038/nrmicro1326.
2. **White JM, Delos SE, Brecher M, Schornberg K.** 2008. Structures and mechanisms of viral membrane fusion proteins: multiple variations on a common theme. Crit. Rev. Biochem. Mol. Biol. **43:**189–219. http://dx.doi.org/10.1080/10409230802058320.
3. **Harrison SC.** 2008. Viral membrane fusion. Nat. Struct. Mol. Biol. **15:**690–698. http://dx.doi.org/10.1038/nsmb.1456.
4. **Wilson I, Skehel J.** 1981. Structure of the haemagglutinin membrane glycoprotein of influenza virus at 3 A resolution. Nature **289:**366–373. http://dx.doi.org/10.1038/289366a0.
5. **Bullough P, Hughson F, Skehel J, Wiley D.** 1994. Structure of influenza haemagglutinin at the pH of membrane fusion. Nature **371:**37–43. http://dx.doi.org/10.1038/371037a0.
6. **Kemble GW, Bodian DL, Rosé J, Wilson IA, White JM.** 1992. Intermonomer disulfide bonds impair the fusion activity of influenza virus hemagglutinin. J. Virol. **66:**4940–4950.
7. **Godley L, Pfeifer J, Steinhauer D, Ely B, Shaw G, Kaufmann R,**

Suchanek E, Pabo C, Skehel JJ, Wiley DC. 1992. Introduction of intersubunit disulfide bonds in the membrane-distal region of the influenza hemagglutinin abolishes membrane fusion activity. Cell **68:**635–645. http://dx.doi.org/10.1016/0092-8674(92)90140-8.

8. **Huang Q, Opitz R, Knapp E-W, Herrmann A.** 2002. Protonation and stability of the globular domain of influenza virus hemagglutinin. Biophys. J. **82:**1050–1058. http://dx.doi.org/10.1016/S0006-3495(02)75464-7.
9. **Böttcher C, Ludwig K, Herrmann A, Heel Van M, Stark H.** 1999. Structure of influenza haemagglutinin at neutral and at fusogenic pH by electron cryo-microscopy. FEBS Lett. **463:**255–259. http://dx.doi.org/10.1016/S0014-5793(99)01475-1.
10. **Kampmann T, Mueller DS, Mark AE, Young PR, Kobe B.** 2006. The role of histidine residues in low-pH-mediated viral membrane fusion. Structure **14:**1481–1487. http://dx.doi.org/10.1016/j.str.2006.07.011.
11. **Stevens J, Corper AL, Basler CF, Taubenberger JK, Palese P, Wilson IA.** 2004. Structure of the uncleaved human H1 hemagglutinin from the extinct 1918 influenza virus. Science **303:**1866–1870. http://dx.doi.org/10.1126/science.1093373.
12. **Stevens J, Blixt O, Tumpey TM, Taubenberger JK, Paulson JC, Wilson IA.** 2006. Structure and receptor specificity of the hemagglutinin from an H5N1 influenza virus. Science **312:**404–410. http://dx.doi.org/10.1126/science.1124513.
13. **Thoennes S, Li Z-N, Lee B-J, Langley WA, Skehel JJ, Russell RJ, Steinhauer DA.** 2008. Analysis of residues near the fusion peptide in the influenza hemagglutinin structure for roles in triggering membrane fusion. Virology **370:**403–414. http://dx.doi.org/10.1016/j.virol.2007.08.035.
14. **Warwicker J.** 1989. A theoretical study of the acidification of the rhinovirus capsid. FEBS Lett. **257:**403–407. http://dx.doi.org/10.1016/0014-5793(89)81582-0.
15. **Warwicker J.** 1992. Model for the differential stabilities of rhinovirus and poliovirus to mild acidic pH, based on electrostatics calculations. J. Mol. Biol. **223:**247–257. http://dx.doi.org/10.1016/0022-2836(92)90729-4.
16. **Grimsley GR, Scholtz JM, Pace CN.** 2009. A summary of the measured pK values of the ionizable groups in folded proteins. Protein Sci. **18:**247–251. http://dx.doi.org/10.1002/pro.19.
17. **Pace CN, Grimsley GR, Scholtz JM.** 2009. Protein ionizable groups: pK values and their contribution to protein stability and solubility. J. Biol. Chem. **284:**13285–13289. http://dx.doi.org/10.1074/jbc.R800080200.
18. **Reed ML, Yen H-L, DuBois RM, Bridges OA, Salomon R, Webster RG, Russell CJ.** 2009. Amino acid residues in the fusion peptide pocket regulate the pH of activation of the H5N1 influenza virus hemagglutinin protein. J. Virol. **83:**3568–3580. http://dx.doi.org/10.1128/JVI.02238-08.
19. **Kalani MR, Moradi A, Moradi M, Tajkhorshid E.** 2013. Characterizing a histidine switch controlling pH-dependent conformational changes of the influenza virus hemagglutinin. Biophys. J. **105:**993–1003. http://dx.doi.org/10.1016/j.bpj.2013.06.047.
20. **Leikina E, Ramos C, Markovic I, Zimmerberg J, Chernomordik LV.** 2002. Reversible stages of the low-pH-triggered conformational change in influenza virus hemagglutinin. EMBO J. **21:**5701–5710. http://dx.doi.org/10.1093/emboj/cdf559.
21. **Fontana J, Cardone G, Heymann JB, Winkler DC, Steven AC.** 2012. Structural changes in Influenza virus at low pH characterized by cryo-electron tomography. J. Virol. **86:**2919–2929. http://dx.doi.org/10.1128/JVI.06698-11.
22. **DuBois R, Zaraket H, Reddivari M, Heath R, White S, Russell C.** 2011. Acid stability of the hemagglutinin protein regulates H5N1 influenza virus pathogenicity. PLoS Pathog. **7:**e1002398. http://dx.doi.org/10.1371/journal.ppat.1002398.
23. **Zaraket H, Bridges OA, Russell CJ.** 2013. The pH of activation of the hemagglutinin protein regulates H5N1 influenza virus replication and pathogenesis in mice. J. Virol. **87:**4826–4834. http://dx.doi.org/10.1128/JVI.03110-12.
24. **Reed ML, Bridges OA, Seiler P, Kim J-K, Yen H-L, Salomon R, Govorkova EA, Webster RG, Russell CJ.** 2010. The pH of activation of the hemagglutinin protein regulates H5N1 influenza virus pathogenicity and transmissibility in ducks. J. Virol. **84:**1527–1535. http://dx.doi.org/10.1128/JVI.02069-09.
25. **Zaraket H, Bridges O a, Duan S, Baranovich T, Yoon S-W, Reed ML, Salomon R, Webby RJ, Webster RG, Russell CJ.** 2013. Increased acid stability of the hemagglutinin protein enhances H5N1 influenza virus growth in the upper respiratory tract but is insufficient for transmission in ferrets. J. Virol. **87:**9911–9922. http://dx.doi.org/10.1128/JVI.01175-13.
26. **Russell CJ.** 11 July 2014. Acid-induced membrane fusion by the hemagglutinin protein and its role in influenza virus biology. Curr. Top. Microbiol. Immunol. http://dx.doi.org/10.1007/82_2014_393.
27. **Stech J, Stech O, Herwig A, Altmeppen H, Hundt J, Gohrbandt S, Kreibich A, Weber S, Klenk H-D, Mettenleiter TC.** 2008. Rapid and reliable universal cloning of influenza A virus genes by target-primed plasmid amplification. Nucleic Acids Res. **36:**e139. http://dx.doi.org/10.1093/nar/gkn646.
28. **Czudai-Matwich V, Schnare M, Pinkenburg O.** 2013. A simple and fast system for cloning influenza A virus gene segments into pHW2000- and pCAGGS-based vectors. Arch. Virol. **158:**2049–2058. http://dx.doi.org/10.1007/s00705-013-1697-4.
29. **Kozerski C, Ponimaskin E, Schroth-Diez B, Schmidt MF, Herrmann A.** 2000. Modification of the cytoplasmic domain of influenza virus hemagglutinin affects enlargement of the fusion pore. J. Virol. **74:**7529–7537. http://dx.doi.org/10.1128/JVI.74.16.7529-7537.2000.
30. **Schroth-Diez B, Ponimaskin E, Reverey H, Schmidt MF, Herrmann A.** 1998. Fusion activity of transmembrane and cytoplasmic domain chimeras of the influenza virus glycoprotein hemagglutinin. J. Virol. **72:**133–141.
31. **Kaverin NV, Rudneva IA, Govorkova EA, Timofeeva TA, Shilov AA, Kochergin-Nikitsky KS, Krylov PS, Webster RG.** 2007. Epitope mapping of the hemagglutinin molecule of a highly pathogenic H5N1 influenza virus by using monoclonal antibodies. J. Virol. **81:**12911–12917. http://dx.doi.org/10.1128/JVI.01522-07.
32. **MacKerell AD, Bashford D, Bellott M, Dunbrack RL, Evanseck D, Field M, Fischer S, Gao J, Guo H, Ha S, Joseph-McCarthy D, Kuchnir L, Kuczera K, Lau F, Mattos C, Michnick S, Ngo T, Nguyen DT, Prodhom B, Reiher W, Roux B, Schlenkrich M, Smith JC, Stote R, Straub J, Watanabe M, Wiórkiewicz-Kuczera J, Yin D, Karplus M.** 1998. All-atom empirical potential for molecular modeling and dynamics studies of proteins. J. Phys. Chem. B **102:**3586–3616. http://dx.doi.org/10.1021/jp973084f.
33. **Im W, Lee MS, Brooks CL.** 2003. Generalized born model with a simple smoothing function. J. Comput. Chem. **24:**1691–1702. http://dx.doi.org/10.1002/jcc.10321.
34. **Kieseritzky G, Knapp E-W.** 2008. Optimizing pKa computation in proteins with pH adapted conformations. Proteins **71:**1335–1348. http://dx.doi.org/10.1002/prot.21820.
35. **Daniels R, Downie J, Hay A.** 1985. Fusion mutants of the influenza virus hemagglutinin glycoprotein. Cell **40:**431–439. http://dx.doi.org/10.1016/0092-8674(85)90157-6.
36. **Herfst S, Schrauwen EJA, Linster M, Chutinimitkul S, de Wit E, Munster VJ, Sorrell EM, Bestebroer TM, Burke DF, Smith DJ, Rimmelzwaan GF, Osterhaus AD, Fouchier RAM.** 2012. Airborne transmission of influenza A/H5N1 virus between ferrets. Science **336:**1534–1541. http://dx.doi.org/10.1126/science.1213362.
37. **Zhang W, Shi Y, Lu X, Shu Y, Qi J, Gao GF.** 2013. An airborne transmissible avian influenza H5 hemagglutinin seen at the atomic level. Science **340:**1463–1467. http://dx.doi.org/10.1126/science.1236787.
38. **Lim AP, Wong SK, Chan AH, Chan CE, Ooi EE, Hanson BJ.** 2008. Epitope characterization of the protective monoclonal antibody VN04-2 shows broadly neutralizing activity against highly pathogenic H5N1. Virol. J. **5:**80. http://dx.doi.org/10.1186/1743-422X-5-80.
39. **Rachakonda PS, Veit M, Korte T, Ludwig K, Böttcher C, Huang Q, Schmidt MFG, Herrmann A.** 2007. The relevance of salt bridges for the stability of the influenza virus hemagglutinin. FASEB J. **21:**995–1002. http://dx.doi.org/10.1096/fj.06-7052hyp.
40. **Puri A, Booy FP, Doms RW, White JM, Blumenthal R.** 1990. Conformational changes and fusion activity of influenza virus hemagglutinin of the H2 and H3 subtypes: effects of acid pretreatment. J. Virol. **64:**3824–3832.
41. **Gruenke JA, Armstrong RT, Newcomb WW, Brown JC, White JM.** 2002. New insights into the spring-loaded conformational change of influenza virus hemagglutinin. J. Virol. **76:**4456–4466. http://dx.doi.org/10.1128/JVI.76.9.4456-4466.2002.
42. **Kalthoff D, Globig A, Beer M.** 2010. (Highly pathogenic) avian influenza as a zoonotic agent. Vet. Microbiol. **140:**237–245. http://dx.doi.org/10.1016/j.vetmic.2009.08.022.
43. **Guan Y, Poon LL, Cheung CY, Ellis TM, Lim W, Lipatov AS, Chan KH, Sturm-Ramirez KM, Cheung CL, Leung YH, Yuen KY, Webster RG, Peiris JS.** 2004. H5N1 influenza: a protean pandemic threat. Proc. Natl. Acad. Sci. U. S. A. **101:**8156–8161. http://dx.doi.org/10.1073/pnas.0402443101.
44. **Qin Z-L, Zheng Y, Kielian M.** 2009. Role of conserved histidine residues in the low-pH dependence of the Semliki Forest virus fusion protein. J. Virol. **83:**4670–4677. http://dx.doi.org/10.1128/JVI.02646-08.

45. **Boo I, te Wierik K, Douam F, Lavillette D, Poumbourios P, Drummer HE.** 2012. Distinct roles in folding, CD81 receptor binding and viral entry for conserved histidine residues of hepatitis C virus glycoprotein E1 and E2. Biochem. J. **443:**85–94. http://dx.doi.org/10.1042/BJ20110868.
46. **Nelson S, Poddar S, Lin T-Y, Pierson TC.** 2009. Protonation of individual histidine residues is not required for the pH-dependent entry of West Nile virus: evaluation of the "histidine switch" hypothesis. J. Virol. **83:** 12631–12635. http://dx.doi.org/10.1128/JVI.01072-09.
47. **Fritz R, Stiasny K, Heinz FX.** 2008. Identification of specific histidines as pH sensors in flavivirus membrane fusion. J. Cell Biol. **183:**353–361. http://dx.doi.org/10.1083/jcb.200806081.
48. **Chanel-Vos C, Kielian M.** 2004. A conserved histidine in the ij loop of the Semliki Forest virus E1 protein plays an important role in membrane fusion. J. Virol. **78:**13543–13552. http://dx.doi.org/10.1128/JVI.78.24.13543-13552.2004.
49. **Zhang W, Shi Y, Lu X, Shu Y, Qi J, Gao GF.** 2013. Supplemental information: an airborne transmissible avian influenza H5 hemagglutinin seen at the atomic level. Science **340:**1463–1467. http://dx.doi.org/10.1126/science.1236787.
50. **Sun X, Shi Y, Lu X, He J, Gao F, Yan J, Qi J, Gao GF.** 2013. Bat-derived influenza hemagglutinin H17 does not bind canonical avian or human receptors and most likely uses a unique entry mechanism. Cell Rep. **3:**769–778. http://dx.doi.org/10.1016/j.celrep.2013.01.025.
51. **Wu Y, Wu Y, Tefsen B, Shi Y, Gao GF.** 2014. Bat-derived influenza-like viruses H17N10 and H18N11. Trends Microbiol. **22:**183–191. http://dx.doi.org/10.1016/j.tim.2014.01.010.
52. **Lu X, Qi J, Shi Y, Wang M, Smith DF, Heimburg-Molinaro J, Zhang Y, Paulson JC, Xiao H, Gao GF.** 2013. Structure and receptor binding specificity of hemagglutinin H13 from avian influenza A virus H13N6. J. Virol. **87:**9077–9085. http://dx.doi.org/10.1128/JVI.00235-13.
53. **Zhu X, Yu W, McBride R, Li Y, Chen L-M, Donis RO, Tong S, Paulson JC, Wilson IA.** 2013. Hemagglutinin homologue from H17N10 bat influenza virus exhibits divergent receptor-binding and pH-dependent fusion activities. Proc. Natl. Acad. Sci. U. S. A. **110:**1458–1463. http://dx.doi.org/10.1073/pnas.1218509110.
54. **Nakowitsch S, Wolschek M, Morokutti A, Ruthsatz T, Krenn BM, Ferko B, Ferstl N, Triendl A, Muster T, Egorov A, Romanova J.** 2011. Mutations affecting the stability of the haemagglutinin molecule impair the immunogenicity of live attenuated H3N2 intranasal influenza vaccine candidates lacking NS1. Vaccine **29:**3517–3524. http://dx.doi.org/10.1016/j.vaccine.2011.02.100.
55. **Krenn BM, Egorov A, Romanovskaya-Romanko E, Wolschek M, Nakowitsch S, Ruthsatz T, Kiefmann B, Morokutti A, Humer J, Geiler J, Cinatl J, Michaelis M, Wressnigg N, Sturlan S, Ferko B, Batishchev OV, Indenbom AV, Zhu R, Kastner M, Hinterdorfer P, Kiselev O, Muster T, Romanova J.** 2011. Single HA2 mutation increases the infectivity and immunogenicity of a live attenuated H5N1 intranasal influenza vaccine candidate lacking NS1. PLoS One **6:**e18577. http://dx.doi.org/10.1371/journal.pone.0018577.
56. **Murakami S, Horimoto T, Ito M, Takano R, Katsura H, Shimojima M, Kawaoka Y.** 2012. Enhanced growth of influenza vaccine seed viruses in Vero cells mediated by broadening the optimal pH range for virus membrane fusion. J. Virol. **86:**1405–1410. http://dx.doi.org/10.1128/JVI.06009-11.
57. **Mair CM, Ludwig K, Herrmann A, Sieben C.** 2014. Receptor binding and pH stability: how influenza A virus hemagglutinin affects host-specific virus infection. Biochim. Biophys. Acta **1838:**1153–1168. http://dx.doi.org/10.1016/j.bbamem.2013.10.004.
58. **Imai M, Watanabe T, Hatta M, Das SC, Ozawa M, Shinya K, Zhong G, Hanson A, Katsura H, Watanabe S, Li C, Kawakami E, Yamada S, Kiso M, Suzuki Y, Maher EA, Neumann G, Kawaoka Y.** 2012. Experimental adaptation of an influenza H5 HA confers respiratory droplet transmission to a reassortant H5 HA/H1N1 virus in ferrets. Nature **486:**420–428. http://dx.doi.org/10.1038/nature10831.